

# Are Argon and Nitrogen Gases Really Inert to Graphene Devices?

Jeevesh Kumar and Mayank Shrivastava

Department of Electronic Systems Engineering, Indian Institute of Science, Bangalore, Karnataka, 560012, India;

E-mail: [mayank@iisc.ac.in](mailto:mayank@iisc.ac.in); [jeevesh@iisc.ac.in](mailto:jeevesh@iisc.ac.in)

**Abstract**— Argon and Nitrogen in their gaseous state are used to provide an inert environment either during probing electronic materials and devices or processing such devices. Although these gases are relatively inert with bulk materials, the gases, however, can interact with different surfaces and influence device physics and surface chemistry. Graphene, a monolayer 2D material, can be influenced by these gases, especially in carbon vacancy and Stone Wales (SW) point defects, which are inherently present in graphene due to growth or synthesis challenges. In this work, we have explored the interaction of graphene with argon and nitrogen in the presence of carbon vacancy and SW point defects based on Density Functional Theory (DFT) and Non-Equilibrium Greens Function (NEGF) computational methods using the QuantumATK simulation tool. We have investigated that, although nitrogen and argon are inert to pristine graphene, the gases enhance their orbitals overlap with graphene in the presence of these defects. Fundamental properties of graphene which drive corresponding device behavior, like band structure, trap states, and fermi energy level, are perturbed by this enhanced interaction. NEGF study reveals that channel current in graphene devices can be degraded due to the influence of these gases in the presence of carbon vacancy and SW defects.

## I. INTRODUCTION

Due to its extraordinary properties, graphene is one of the leading candidates among the 2D materials that can replace silicon in the future generation of electronic devices [1]. However, the properties of graphene can be degraded due to its various defects [2]. Carbon vacancy and Stone Wales (SW) are major point defects inherently present in graphene due to existing challenges in its growth or synthesis [3]. Interaction of graphene with external agents can be enhanced by these defects by enhancement in their orbitals overlap [4]-[6]. Nitrogen (N<sub>2</sub>) and argon (Ar) gases, which are generally used for inert environments, can also perturb the properties of graphene in the presence of such defects. Thus, it is worth investigating the influence of nitrogen and argon on graphene in the presence of carbon vacancy and SW defects to understand their degree of inertness. Using DFT and NEGF, we have investigated the influence of argon and nitrogen on graphene in the presence of carbon vacancy and SW defects. This manuscript has discussed defect-assisted orbital overlap enhancement of graphene with these gases. We have also highlighted how graphene's fundamental properties like band structure, Fermi energy level, and trap states are perturbed by these orbital overlap enhancements. Finally, we have elaborated deterioration in different properties, like transmission spectrum, device density of state, and channel current, of graphene devices with the defects under the influence of argon and nitrogen. Our work can give insights into the degradation in properties of graphene devices by the inert environment maintained by argon or nitrogen gases.

## II. COMPUTATIONAL DETAILS

QuantumATK package was used for all the computations [6]. A 7x7 supercell each of (i) pristine graphene, (ii) graphene with single carbon vacancy (vac-graphene), and (iii) graphene with single Stone Wales defect (SW-graphene), and the same modules with gas molecules (Fig. 1) were optimized for their minimum energy. Energy optimizations were done with 0.01 eV/Å force and 0.001 eV/Å<sup>3</sup> energy cutoffs. Perdew-Burke-Ernzerhof (PBE) form of generalized gradient approximation (GGA) functional and Grimme-D2 Van der Waals (vdW) correction were used in computations with 5x5x1 k point sampling. Periodic boundary conditions were applied in all the bulk calculations to emulate a large area graphene monolayer. ~30 Å vacuum region was added in the supercells perpendicular to the graphene plane to nullify interlayer interactions. For device calculation using NEGF, the length and width of all graphene device channels were ~36.9 Å and ~12.8 Å, respectively. Ideal electrodes and 5x500 k-point sampling were used in all the device computations

## III. RESULTS AND DISCUSSION

Optimized C-C (~1.43 Å) and N-N (~1.43 Å) bond lengths are close to the previously reported values, which validates our computational approach and parameters used for further exploration and analysis.

**Optimum bond distances and Energies:** Optimum distance of argon (Ar) from pristine, vac-graphene and SW-graphene are ~3.54 Å, 3.53 Å, and 3.56 Å, and corresponding negative interactions energies are ~5.52 eV, ~5.38 eV and ~5.59 eV respectively (Fig. 2). For N<sub>2</sub>, corresponding distances and energies are ~3.14 Å, ~3.24 Å and ~3.29 Å, and ~5.53 eV, ~5.66 eV and ~5.89 eV, respectively. Negative interaction energies of all the modules tell that the interactions are thermodynamically favorable. However, the interactions are in long-range vdW regimes due to more than 3 Å optimum interaction distances in all the conditions. We need to further explore the strength of the interactions in terms of orbitals overlap.

**Defect-assisted orbitals overlap:** Electron densities (ED) in the bonding regimes of graphene with N<sub>2</sub> and Ar are increased significantly due to SW defects in graphene (Fig. 3). Carbon vacancy also increases ED in the bonding regimes of graphene with N<sub>2</sub>. The electron densities increments tell that orbitals overlap between graphene and gas molecules are enhanced by these defects in the graphene. This defect-assisted orbitals overlap can perturb fundamentals properties of graphene due to rehybridizations in corresponding wave functions by the gaseous interactions.

**Perturbation in fundamental properties:** Ar and N<sub>2</sub> don't disturb band structures of pristine graphene (Fig. 4). However, the gases perturb mid gap (trap) states energy levels of vac-graphene. The gases also drift fermi level towards the valance band. Thus, Ar and N<sub>2</sub> enhance the p-type behavior of graphene in the presence of carbon vacancy. The bandgap of SW graphene is enlarged from ~0.05 eV to ~0.06 eV and ~0.08 eV by Ar and N<sub>2</sub>, respectively. Due to perturbation in these properties, especially fermi level and trap states, graphene device properties can be influenced under Ar and N<sub>2</sub> when it has significant carbon vacancy and/or SW defects.

**Degradation in device properties:** We have explored corresponding device behaviors by analyzing of transmission spectrum (Fig. 5), device density of states (Fig. 6), and current-voltage characteristics (Fig. 7) in suspended conditions under Ar and N<sub>2</sub> molecules. Transmission spectrum (TS) and device density of states (DDOS) near the Fermi levels of vac-graphene are reduced by Ar (5b & 6b) and N<sub>2</sub> (5e & 6e). Thus, the effective carrier concentration in the vac-graphene channel is reduced by Ar and N<sub>2</sub>. Due to a reduction in the carrier concentration, channel current in the vac-graphene is reduced significantly (Fig. 7b) in the presence of Ar and N<sub>2</sub> molecules. Channel current in pristine graphene (Fig. 7a) doesn't change because corresponding TS (5a & 5d) and DDOS (6a & 6d) are not disturbed by these gases significantly. For SW graphene, device current (Fig. 7c) changes marginally due to marginal change in the TS (5c & 5f) and DDOS (6c & 6f) near the Fermi level.

## IV. CONCLUSION

In conclusion, Ar and N<sub>2</sub> interact significantly with graphene in the presence of carbon vacancy and SW defects. Although, these gases stay in vdW regimes over graphene. Their orbitals overlap, however, enhanced by these defects. The orbitals overlap perturbs some of its fundamental properties like band structures, trap states, and fermi energy levels of graphene. Such perturbation, especially fermi level and trap states, reduces effective carrier concentration in its device due to reduced carrier transmission probabilities and device density of states, especially for vac-graphene. The reduction in carrier concentration under these gases reduces the channel current of graphene with carbon vacancies. Ar and N<sub>2</sub> don't change the channel current of pristine graphene. However, they influence the channel current of graphene marginally in the presence of SW defects. Since carbon vacancies and SW defects are present in graphene inherently due to its growth/synthesis limitations, we can say that Ar and N<sub>2</sub> gas doesn't provide a completely inert environment for graphene.

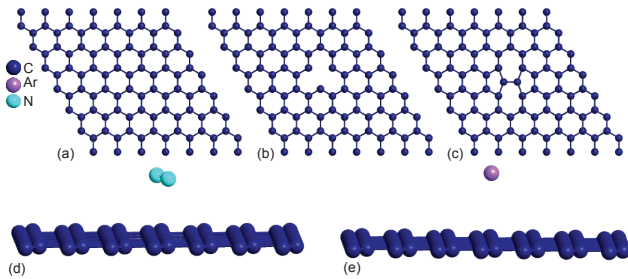


Figure 1: 7x7 super cell of (a) pristine graphene, (b) graphene with 1-C atom vacancy (vac. graphene) and (c) graphene with one Stone Wales defect (SW graphene). Optimized minimum energy super cell module of (d) pristine graphene-N<sub>2</sub> system and (e) pristine graphene-Ar system. Similar modules have been simulated for vac. graphene and SW graphene as well.

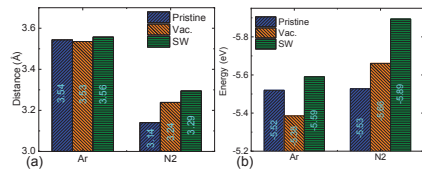


Figure 2: (a) Distance of Ar and N<sub>2</sub> with different graphene surfaces and (b) corresponding change in energy, when energy minima are achieved.

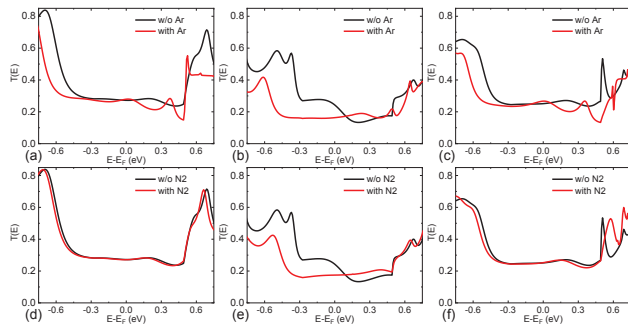


Figure 5: Transmission spectrum (TS) comparison of (a) pristine graphene, (b) vac. graphene and (c) SW graphene with and without Ar as well as (d) pristine graphene, (e) vac. graphene and (f) SW graphene with and without N<sub>2</sub>. Fermi energy is at zero energy level. Ar and N<sub>2</sub> reduce transmission probability of electron in graphene channel near Fermi level. Effect is significant for vac. graphene (b & e). Ar reduces TS more than N<sub>2</sub> in respective graphene channels.

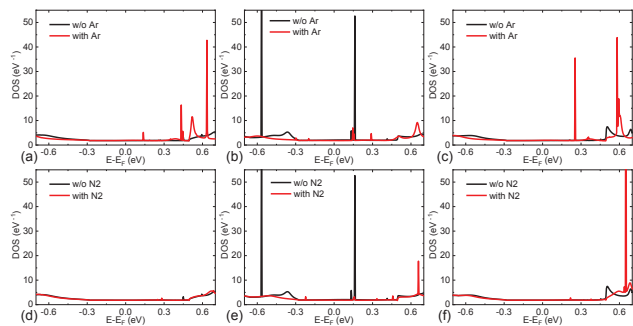


Figure 6: Device Density of States (DDOS) comparison of (a) pristine graphene, (b) vac. graphene and (c) SW graphene with and without Ar as well as (d) pristine graphene, (e) vac. graphene and (f) SW graphene with and without N<sub>2</sub>. Fermi energy is at zero energy level. Ar and N<sub>2</sub> do not change, reduce and increase DDOS near Fermi level of pristine graphene (a, d), vac. graphene (b, e) and SW graphene (c, f) respectively.

**REFERENCES:** [1] R. Frisenda *et al.* npj 2D Mater Appl 4, 38 (2020). [2] F. Banhart *et al.* ACS nano 5, no. 1 (2011): 26-41. [3] Tian *et al.* Micromachines 8, no. 5 (2017): 163. [4] D. W. Boukhvalov *et al.*, Nano letters 8, no. 12 (2008): 4373-4379. [5] F. Ricciardella *et al.*, Nanoscale 9, no. 18 (2017): 6085-6093. [6] J. Kumar *et al.*, ACS Omega 2020, 5, 48, 31281-31288. [7] QuantumATK, version 2018.6.

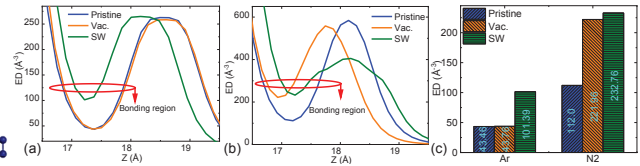


Figure 3: Electron Density (ED) in the bonding regime (between surface and gas molecules) of (a) graphene-Ar system and (b) graphene-N<sub>2</sub> system. (c) minimum ED in the bonding regimes of all the interacting systems. Minimum ED in the bonding regime is increasing due to Stone Wales (SW) in graphene. This means, SW defect enhances orbital overlaps of graphene with Ar and N<sub>2</sub>. Carbon vacancy also increases orbital overlaps of graphene with N<sub>2</sub> significantly.

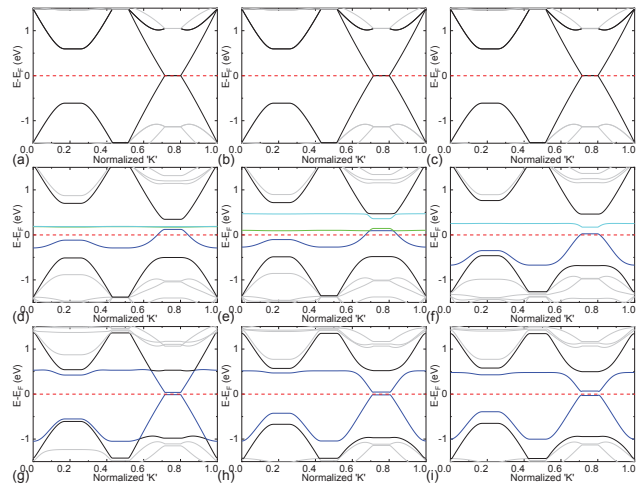


Figure 4: Band structure of (a) pristine graphene only, (b) pristine graphene-Ar, (c) pristine graphene-N<sub>2</sub>, (d) vac. graphene only, (e) vac. graphene-Ar, (f) vac. graphene-N<sub>2</sub>, (g) SW graphene only, (h) SW graphene-Ar and (i) SW graphene-N<sub>2</sub>. Ar and N<sub>2</sub> do not disturb band structure of pristine graphene. Both perturb degenerate mid-gap (trap) states of vac. graphene and enhance p-type behavior in graphene by moving Fermi level  $\sim 0.01$  eV and  $\sim 0.12$  away from conduction band respectively. Ar splits the degenerate trap states and moves one trap state near conduction band. One of the degenerate trap states is disappeared from the mid gap region due to N<sub>2</sub>. Ar and N<sub>2</sub> increase band gap of SW graphene from  $\sim 0.05$  eV to  $\sim 0.06$  eV and  $\sim 0.08$  eV respectively. All the band structures are plotted with normalized 'k' which is along G  $\rightarrow$  M  $\rightarrow$  L  $\rightarrow$  A  $\rightarrow$  G  $\rightarrow$  K  $\rightarrow$  H  $\rightarrow$  A. Position of G, M, L, A, G, K, H, and A points on the k axis are 0, 0.172, 0.258, 0.430, 0.516, 0.715, 0.801 and 1.0 respectively. Fermi energy has been set to zero energy level in all the band structure plots.

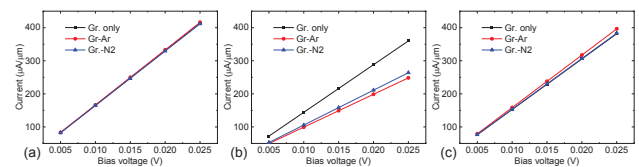


Figure 7: Current vs applied bias voltage comparison of suspended graphene simulating device without any gate voltage under Ar and N<sub>2</sub> gases. (a) comparison of pristine graphene, (b) comparison of vac. graphene, (c) comparison of SW graphene. channel length and width are 36.918 Å and 12.789 Å respectively. Ar and N<sub>2</sub> do not influence current in pristine graphene (a). they reduce current through vac. graphene (b), where N<sub>2</sub> influences more than Ar. For SW graphene, Ar increase the current marginally (c).